Spatially resolved electronic detection of biopolymers

F. Pouthas,[1] C. Gentil,[1] D. Côte,[1] G. Zeck,[2] B. Straub,[2] and U. Bockelmann[1,*]
[1]*Laboratoire Pierre Aigrain, Département de Physique de l'Ecole Normale Supérieure, 24 rue Lhomond, 75005 Paris, France*
[2]*Max Planck Institut für Biochemie, D-82152 Martinsried, Germany*
(Received 13 February 2004; published 21 September 2004)

An integrated array of field-effect transistor structures is used to detect two oppositely charged biopolymers: poly(L-lysine) and DNA. Local deposition of polymer solutions on part of the array induces sizeable variations in the dc current-voltage characteristics of the transistors exposed to the molecular charge. The whole transistor array is measured in the presence of a common electrolyte. Differential signals are studied as a function of electrolyte salt and polymer concentrations. The measurements provide information on the interface electrostatic potentials of the (semiconductor/biopolymer/electrolyte) system and the experimental data are compared to an analytical model which accounts for screening of the adsorbed charge by mobile ions.

DOI: 10.1103/PhysRevE.70.031906 PACS number(s): 87.80.−y

I. INTRODUCTION

Following the pioneering work of Bergveld [1], a considerable research effort was devoted to the electronic detection of biomolecules with semiconductor field-effect devices [2–7]. The approach is attractive because it allows for label-free detection and could lead to a powerful interface between molecular biology and microelectronics. The detection principle involves immobilization of a charged molecular species on a solid/liquid interface, which causes a shift in electrostatic potential, and, by field effect, modifies the dc conductivity of a buried electron gas. Experimentally, however, it has been found that a change in electrostatic potential of a solid/liquid interface is hard to detect by such dc-field-effect measurement, the difficulty was attributed to electrostatic screening by mobile ions [2]. Most research work thus concentrated on capacitive effects, which are measured as transients or in an ac mode [2–6]. The ac measurements, often called impedance spectrocopy when performed as a function of frequency, are analyzed in terms of equivalent circuits. The latter typically involve several effective capacitance and resistance parameters, which provide a phenomenological description of the solid/liquid interface with the biomolecule layers [8,9].

In this paper, we consider the adsorption of poly(L-lysine), single-stranded and double-stranded DNA to the active regions of a monolytically integrated array of field-effect transistors (FET's). First, adsorption to part of the array is obtained by local deposition with a microspotting device or a micropipet. Afterwards, the dc current-voltage characteristics of all individual FET's are measured, while the entire array is in contact with a common electrolyte solution. A sizeable and reproducible variation of the characteristics is observed for the transistors that have been exposed to the molecular charge.

The paper is organized as follows. In Sec. II, the principle and the setup of the electronic measurements are presented. Section III contains a simple theoretical description of the semiconductor/biomolecule/electrolyte system. Experimental results on poly(L-lysine) adsorption are considered in Sec. IV. Differential signals are studied as a function of electrolyte salt and poly(L-lysine) concentrations and are compared to the theoretical description. In Sec. V, electronic detection of single- and double-stranded DNA is considered and a comparison to microscopic fluorescence measurements is presented.

In a previous publication, we showed that our electronic measurements are compatible with enzymatic technology and complex genomic DNA samples [7]. We combined the approach with an allele-specific polymerase chain reaction and thus detected a single-base-pair mutation in human DNA.

II. PRINCIPLE AND SETUP OF THE ELECTRONIC MEASUREMENTS

We use arrays of monolithic integrated silicon *p*-channel FET devices (Fig. 1). The gate areas of the individual FET's are not metallized but are, via a locally thinned oxide layer ($d_{SiO_2}=10$ nm), in contact with a common electrolyte solution. With an Ag/AgCl electrode a voltage is applied between the electrolyte and the common source contact. We use two different structures with 62 or 96 FET's, linearly arranged with a period of 20−40 μm and active surface areas of 24, 36, or 40 μm^2. Device fabrication is described in Refs. [10,11].

We measure the drain current I_D as a function of a dc voltage U_{SD} applied between source and drain and a dc voltage U_S applied between source and the reference electrode. These measurements are performed at room temperature for the whole FET array using a custom current amplifier in combination with a commercial I/O board, as presented schematically in Fig. 2. The FET's are multiplexed by a custom switch unit that is computer controlled by a digital I/O board (PCI 6503, National Instruments). Two dc voltages $\tilde{U}_S$, $\tilde{U}_{SD}$ are generated by 16-bit D/A converters of a multifunction I/O board (PCI 6052E, National Instruments) and are low-pass filtered in the input stage of the amplifier. The amplifier

*Author to whom correspondence should be addressed. Email address: ulrich@lpa.ens.fr

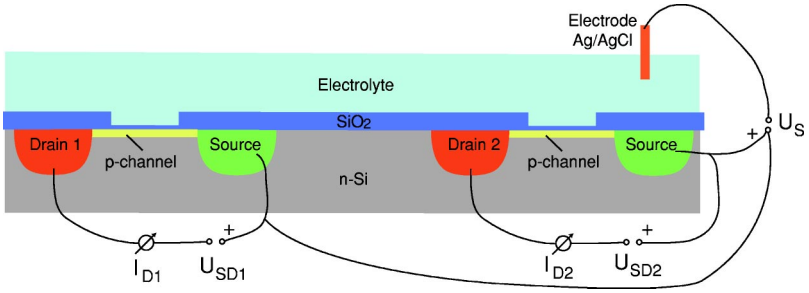

FIG. 1. (Color online) Schematic view of the measurement configuration, showing the cross-section of two *p*-channel transistors from an array of 96. A Ag/AgCl electrode is immersed in an electrolyte liquid that covers the whole transistor array. A voltage U_{SD} is applied between source and drain and a voltage U_S is applied between the source and the Ag/AgCl electrode. The drain current I_D is measured for each transistor of the array as a function of U_{SD} and U_S.

circuit contains a voltage summing amplifier, since the potentials for source and drain are referenced with respect to the potential of the Ag/AgCl electrode. The drain current is converted to a voltage that is measured by a 16 bit A/D converter of the I/O board. Acquisition of the bidimensional current-voltage characteristics $I_D(\tilde{U}_{SD},\tilde{U}_S)$ of all FET's is controlled by computer with software written in the Labwindows/CVI (National Instruments) environment.

In our silicon devices the connections to the individual drains and the common source have been realized by boron p^+ implantation and exhibit a geometrical variation in length and width. This leads to non-negligable serial resistances that vary across the FET array. With the known geometry of the individual connections we can deduce the serial resistances for the drain lead R_D and the source lead R_S of each FET and perform the transformation

$$U_S = \tilde{U}_S - R_S I_D,$$

$$U_{SD} = \tilde{U}_{SD} - (R_D + R_S) I_D.$$

This transformation gives a corrected characteristic $I_D(U_{SD},U_S)$, that to a good approximation, is not affected by the serial resistances. To study the potential shifts in U_S at constant $\{I_D,U_{SD}\}$ we convert the $I_D(U_{SD},U_S)$ characteristics, to $U_S(I_D,U_{SD})$ by numerical interpolation.

III. THEORETICAL DESCRIPTION

The experimental characteristics are $I_D=f(U_{SD},U_S)$. Although not directly related to U_S, the electric field E_{SiO_2} inside the oxide layer is a useful parameter to describe the coupling between the solid state part of the FET ($x<0$) and its aqueous part ($x>0$). We adopt here a simple one-dimensional description, illustrated in Fig. 3, neglecting the lateral variation of E_{SiO_2} from source to drain.

The drain current I_D is thus determined by the values of U_{SD} and E_{SiO_2}. Conversely, if at constant U_{SD} we experimentally impose a fixed value for I_D, the electric field E_{SiO_2} remains constant. Thus the potential drop $\phi_{\text{solid state}}$ between the quasibidimensional hole gas of the inversion layer ($x\leqslant -d$) and the solid-liquid interface ($x=0$) remains also constant, whatever the changes occurring in the aqueous part of the device are.

The SiO_2/electrolyte interface is described by an interface charge σ_{int} followed by a diffuse layer charge. In a simplifying picture, the interface charge σ_{int} can be seen as the sum of two contributions: a negative surface charge σ_1 mainly due to the ionized silanol groups SiO^-, and a positive Helmholtz plane charge σ_2 due to adsorbed cations. As a whole the interface charge $\sigma_{\text{int}}=\sigma_1+\sigma_2$ is still negative [12]. The potential drop across the interface is given by

$$\phi_0 = \phi(0) - \phi(a) = \frac{\sigma_1 + \epsilon_0 \epsilon_r^{SiO_2} E_{SiO_2}}{\epsilon_0 \epsilon_r^{in}} a, \qquad (1)$$

where a is the width of the layer between the surface and the Helmholtz plane and ϵ_r^{in} is its relative dielectric constant

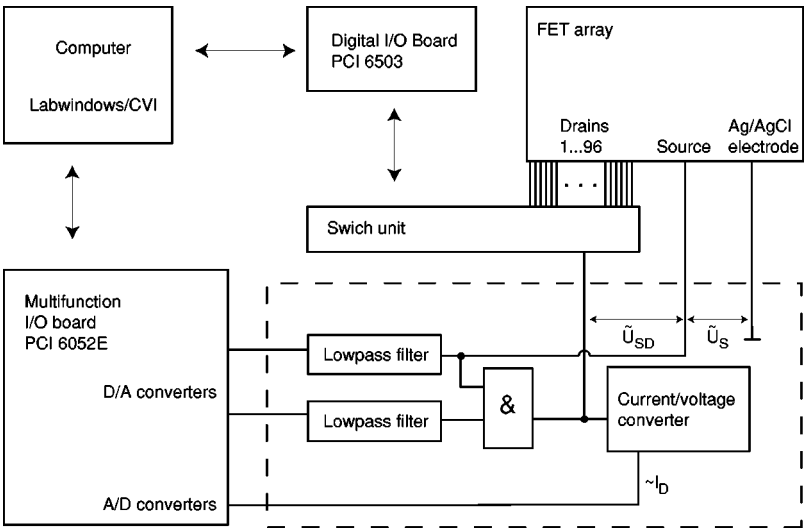

FIG. 2. Recording setup used for the differential detection of biopolymers. The FET array contains one drain connection for each of the 96 transistors and one common source.

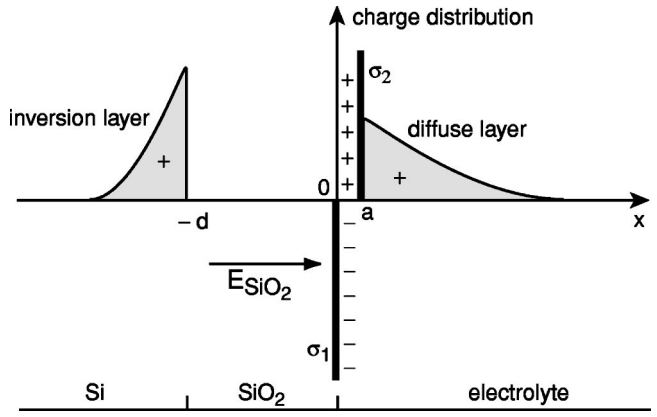

FIG. 3. Schematic representation of the charge distribution assumed in the one-dimensional model of the FET/electrolyte system.

(usually assumed to be smaller than the water bulk value $\epsilon_r^{H_2O}$).

In the diffuse layer, composed of monovalent K^+ and Cl^- ions (KCl 1:1 electrolyte), the potential $\phi(x)$ is described within a Gouy-Chapman model [13]:

$$\phi(x) - \phi(\infty) = \frac{2kT}{e}\text{arsinh}\left[\sqrt{\frac{\epsilon_0\epsilon_r^{H_2O}}{[Cl^-]8kT}}\left(-\frac{d\phi}{dx}\right)\right], \quad (2)$$

where the electric field varies from

$$-\frac{d\phi}{dx}(a) = \frac{\sigma_{\text{int}} + \epsilon_0\epsilon_r^{SiO_2}E_{SiO_2}}{\epsilon_0\epsilon_r^{H_2O}} = \frac{\sigma_{\text{eff}}}{\epsilon_0\epsilon_r^{H_2O}} \quad (3)$$

at the plane ($x=a$), to zero deep inside the electrolyte ($x \gg 0$). The effective charge $\sigma_{\text{eff}}=\sigma_{\text{int}}+\epsilon_0\epsilon_r^{SiO_2}E_{SiO_2}$ is the charge of the SiO_2 surface with the Helmholtz layer of adsorbed cations plus a contribution of the field E_{SiO_2}. The diffuse layer potential difference between the interface and the bulk electrolyte is therefore

$$\phi_1 = \phi(a) - \phi(\infty) = \frac{2kT}{e}\text{arsinh}\left(\frac{\sigma_{\text{eff}}}{\sqrt{[Cl^-]8kT\epsilon_0\epsilon_r^{H_2O}}}\right). \quad (4)$$

At the other solid-liquid interface, the potential between the bulk electrolyte and the bulk silver metal is the opposite of the Nernst potential of the Ag/AgCl electrode [14]:

$$\phi_2 = -\phi_{\text{Nernst}} = \frac{kT}{e}\ln\left(\frac{a(Cl^-)}{a(Cl^-)_{PZC}}\right). \quad (5)$$

In this relation $a(Cl^-)_{PZC}$ denotes the chloride ion activity [15] at the point of zero charge. The voltage U_S between the quasibidimensional hole gas and the bulk silver electrode is therefore equal to

$$U_s = \phi_{\text{solid state}}(E_{SiO_2}) + \phi_0(\sigma_1, E_{SiO_2}) + \phi_1(\sigma_{\text{eff}}, [Cl^-]) + \phi_2([Cl^-]). \quad (6)$$

In order to maintain the current I_{SD} at a constant value, which implies constant electric field E_{SiO_2}, any change in the sum $\phi_0+\phi_1+\phi_2$ induced by a rearrangment of molecular species at the solid/liquid interfaces or in the electrolyte must be compensated by an equal change in the externally applied voltage U_S:

$$\Delta U_S = \Delta\phi_0 + \Delta\phi_1 + \Delta\phi_2. \quad (7)$$

The previous model has been derived for the case of a pure KCl electrolyte. When charged polymers are adsorbed to the SiO_2 surface, we use the same model and fit the experimental variation ΔU_S as a function of salt concentration with two free parameters σ_{eff} and C using the expression

$$\Delta U_S = C + \Delta\phi_1 + \Delta\phi_2. \quad (8)$$

Experimentally, we often observe a non-negligable offset C after biomolecule deposition, which indicates that the molecular adsorption modifies both the Helmholtz layer and the diffuse layer.

Our model, based on a one-dimensional (1D) approximation [16,17], assumes a fixed working point $\{I_D, U_{SD}\}$. Experimentally, a weak dependence on the working point exists, this correction is, however, small compared to the effects of the electrolyte salt and of the effective interface charge σ_{eff}. Therefore the representation of the data in terms of U_s (or ΔU_s) allows us to study the SiO_2/polymer/electrolyte interface without entering into the details of the current-voltage characteristics of the transistor.

IV. ELECTRONIC DETECTION OF POLY(L-LYSINE) ADSORPTION

As a first system for electronic detection of molecular charge, we have chosen the adsorption of poly(L-lysine) to the SiO_2 surface of the device. Poly(L-lysine) presents NH_3^+ groups at neutral *p*H that lead to an electrostatic attraction to glass and SiO_2, which is widely used for immobilization of biomolecules, in particular in the field of DNA microarrays. The thermodynamics of poly(L-lysine) adsorption from a liquid phase to a glass surface has been investigated experimentally and theoretically [18,19].

We first perform a global treatment of the SiO_2 surface: incubation in sulfochromic acid (1–2 min), rinsing with a stream of de-ionized H_2O, incubation in a NaOH/ethanol solution (60 μl NaOH 16 N, 220 μl H_2O, 420 μl ethanol, 3–5 min), H_2O rinsing and drying with air. Afterwards, using a custom microspotting setup equipped with video control, poly(L-lysine) solutions (P8920, Sigma, St. Louis, MO, USA) are locally spotted on the FET array. Unless stated otherwise, poly(L-lysine) dilution is $c_0=0.01\%$ w/v ($\sim$800 μM lysine monomers) in $0.1\times$PBS buffer at *p*H 7. Each spot covers several transistors (Fig. 4). The sample is kept 15 min at room temperature in a humid environment before 5 min drying at 50 °C. The surface is then covered with an electrolyte solution to perform the electronic measurements.

The poly(L-lysine) deposition leads to a decrease in I_D (Fig. 5). Such decrease is expected for adsorption of a positive charge to the *p*-channel device. A decrease in I_D at constant $\{U_S, U_{SD}\}$ corresponds to a positive shift of U_S at constant $\{I_D, U_{SD}\}$. In Fig. 6 two series of measurements at various electrolyte salt concentration [KCl] are shown. Local

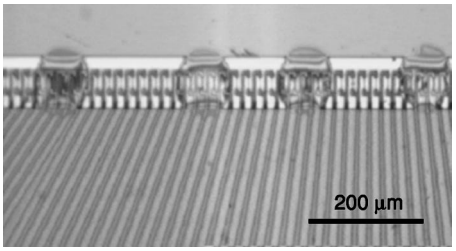

FIG. 4. Image of a FET array with four local deposits. Each spot covers about five adjacent transistor gates. The gray lines in the image mark the individual drain connections. The gray region in the upper part is the common source connection.

deposition of poly(L-lysine) around transistor 7 and transistor 25 induces positive peaks in ΔU_S with heights of about 90 mV at 0.01 mM KCl (bottom curves). Starting at 0.01 mM, a first series (*) of increasing concentration has been obtained by successively adding concentrated KCl solution to the electrolyte. Afterwards the FET array is rinsed with H_2O and a second series (◦) is measured. With increasing [KCl], we reproducibly observe an increase in ΔU_S, accompanied by a progressive weakening of both charge induced peaks.

In Fig. 7 the measured [KCl] dependencies are extracted and compared to the theoretical description. Without adsorbed poly(L-lysine) best agreement between the measured dependence and the calculation is obtained for an effective charge $\sigma_{\text{eff}}=-13\times10^{-4}$ C/m^2. This value is subject to sizable variation ($-13\pm12\times10^{-4}$ C/m^2), as observed by comparing seven salt series measured on different surfaces. The local poly(L-lysine) adsorption typically increases the fitted effective charge to a close to zero value. We obtain $\sigma_{\text{eff}}=-1.0\times10^{-4}$ C/m^2 in the present case and statistically $(2.2\pm4.7)\times10^{-4}$C/m^2 on seven salt series.

In Fig. 8 the dependence of the adsorption induced shift on the concentration of the poly(L-lysine) solution is shown. We observe a rapidly increasing shift followed by a pronounced saturation. We attribute the measured saturation to a limitation in the amount of positively charged polyelectrolytes that can be adsorbed to the globally negative SiO_2/electrolyte interface. Such charge induced limitation of adsorption has been studied theoretically [20] and was used to fabricate layered polymeric multicomposites [21]. Depending on the short range interactions at the interface, polyelectrolyte adsorption is expected to stop slightly before or after reversal of the sign of the interface charge. This could also explain our measurement of close to zero effective charge values after poly(L-lysine) deposition, just described (Fig. 7). In these measurements saturation occurs for poly(L-lysine) concentrations above c_0, which corresponds to $\sim$20 lysines/nm^2 and is thus comparable to the saturation concentration observed for poly (L-lysine) adsorption on glass microspheres [18]. At low concentration, signals measured on pure buffer spots ($\sim$40 mV in Fig. 8) limit our detection range.

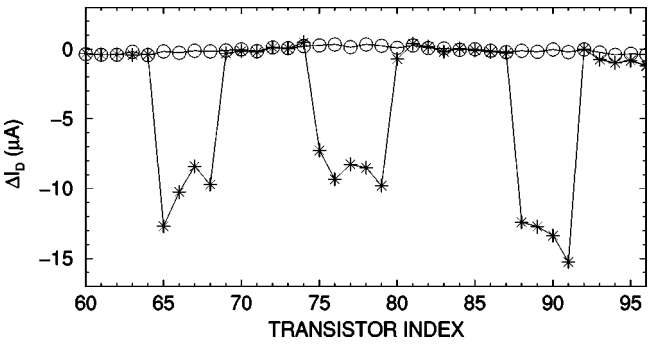

FIG. 5. Detection of poly(L-lysine): Local deposition of poly(L-lysine) induces changes of about 10 μA in the drain current I_D. The I_D measurement is performed before and after deposition of the biopolymer. Sizeable changes depicted by stars are seen only on the poly(L-lysine) covered transistors. For comparison the difference between to subsequent I_D measurements separated by H_2O rinsing is presented as open circles. All measurements are performed at U_S=1 V, U_{SD}=0.9 V in a 0.1-mM KCl electrolyte.

V. ELECTRONIC DETECTION OF DNA

Both single and double stranded DNA molecules carry negative charge in aqueous solution around *p*H 7, opposite to the positively charged poly(L-lysine). Figure 9 illustrates the immobilization and dc-field-effect detection of DNA oligonucleotides. Different from Figs. 6 and 8, we present here directly U_S rather than a voltage difference ΔU_S. After initial NaOH surface treatment a variation in U_S often appears across the array (about 100 mV in this case). To mediate DNA immobilization, we incubate the FET array for 30 min in a poly(L-lysine) dilution (without drying, concentration c_0), followed by H_2O rinsing and drying with air. This incubation leads to positive shifts in U_s by 100 ± 56 mV (statistics based on 105 prepared surfaces) that reduce the FET-to-FET differences in the electronic signal. These shifts are comparable to the values measured on dried local deposits at concentration c_0 (Figs. 6 and 8). The reduction in the FET-to-FET variation can be understood along the same line as the saturation of the poly(L-lysine) peaks: adsorption is expected until the surface acquires a close to zero effective charge. Lateral charge inhomogenity that may be present after the NaOH treatment can be reduced, since a more homogeneous surface of close to zero effective charge is expected for saturating poly(L-lysine) concentrations. Subsequent to the poly(L-lysine) incubation the surface is rinsed with H_2O, dried with air, and fluorescent DNA oligonucleotides are spotted. We keep these deposits at least 15 min in a humid room temperature environment before drying in air. Subsequent electronic measurement reveals distinct DNA induced negative peaks. Opposite to the case of poly(L-lysine), we thus observe negative shifts in U_s for DNA, as expected for the accumulation of a negative additional charge at the solid surface. The local DNA deposition and immobilization is verified with a custom microfluorescence setup, top row of Fig. 9. This fluorescence setup is described in the Appendix.

In Fig. 10, we compare the electronic signals with fluorescence measurements. Cy-5 modified oligonucleotides of increasing concentration and a negative control (KCl, 0.01 mM) are spotted. Each fluorescence data point represents the average intensity measured on the active surface of

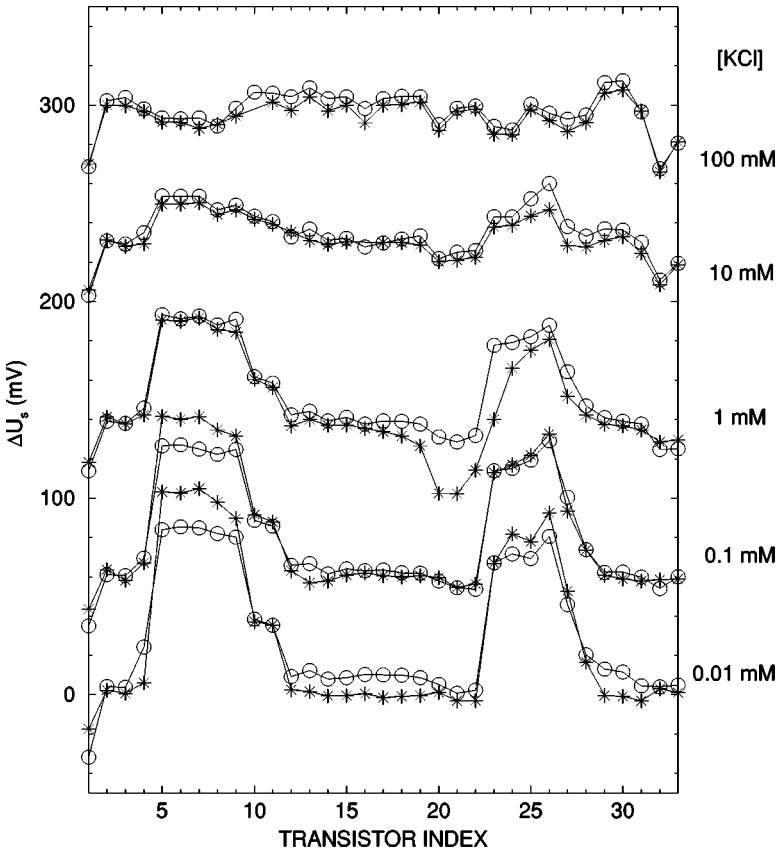

FIG. 6. Voltage differences ΔU_S measured on part of a 62-FET array at $U_{SD}=1.2$ V and $I_D=50$ μA. Differences between a reference measurement (done at 0.01 mM added KCl before local deposition) and two salt concentration series [measured after local depositions of poly(L-lysine)] are presented. Stars correspond to the first concentration series, open circles to the second concentration series.

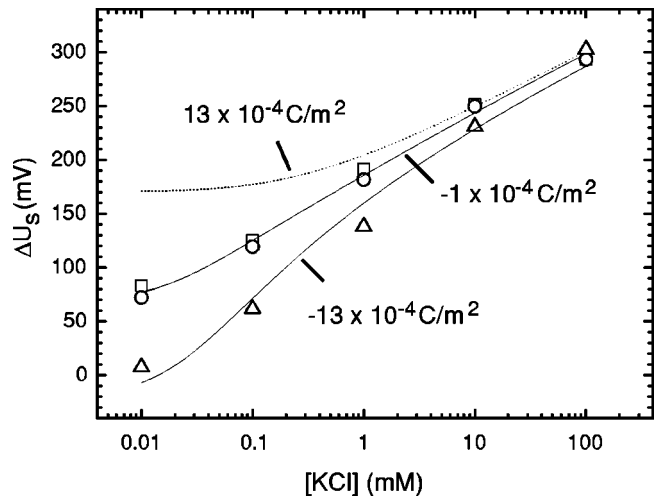

FIG. 7. Voltage difference ΔU_S as a function of electrolyte salt. The experimental points are derived from the data of Fig. 6. Squares and circles correspond to averages of the ΔU_S values measured on the FET's with poly(L-lysine) adsorption (peaks around transistor 7 and 25, respectively), the triangles indicate an average over a set of FET's without added polymers. The theoretical curves are calculated using Eqs. (4) and (5), with different values of σ_{eff}, taking into account partial dissolution of AgCl from the Ag/AgCl electrode at low salt and the concentration dependence of the activity coefficient of a KCl electrolyte. A curve for a positive value of σ_{eff} is shown for comparison.

an individual FET. In the presented concentration range, a clear correlation appears between the electronic and the optical signals. At lower concentrations our electronic detection becomes limited by signals that appear already upon simple deposition of salted buffers. We also find that the electronic signals saturate for oligonucleotide concentrations above 20–50 μM. Comparing different transistor arrays, we observe some variability in the peak heights and in the onset of the saturation. These quantities are expected to depend on the

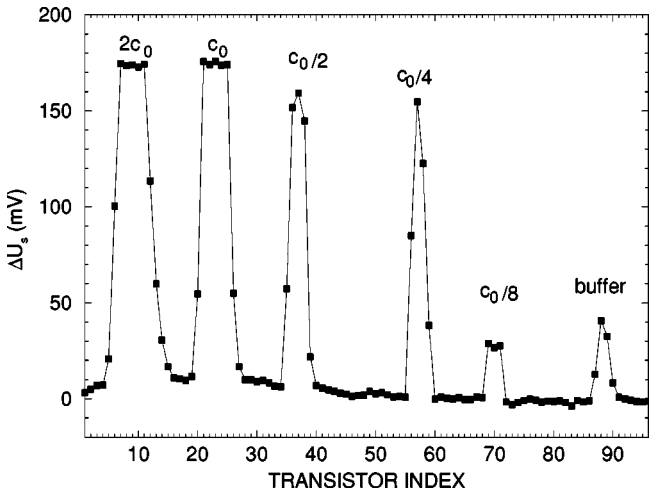

FIG. 8. Field-effect detection of local poly(L-lysine) adsorption for different polymer concentrations. All dilutions are in 0.1 $\times$PBS *p*H 7, the concentration c_0 is given in the text. $U_{SD}=1$ V, $I_D=100$ μA, [KCl]=0.01 mM.

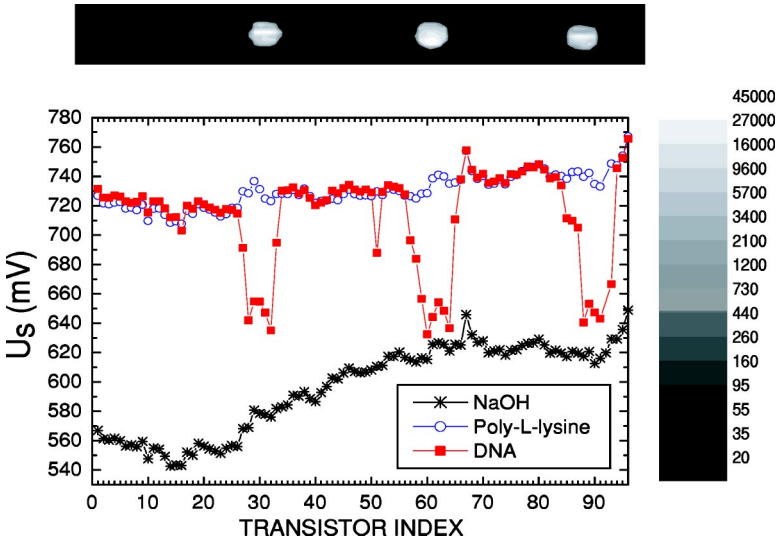

FIG. 9. (Color online) Immobilization and electronic detection of DNA. The voltages U_s corresponding to a given working point (U_{SD} =1 V, I_D=100 μA, [KCl]=0.01 mM) are derived from the measured $I_D(U_S, U_{SD})$ characteristics and are plotted as a function of the transistor index. The same working point applies to Figs. 10 and 11. Crosses: measurement after initial NaOH surface treatment. Circles: measurement subsequent to poly(L-lysine) incubation of the whole array. Squares: measured after local deposition of DNA oligonucleotides (5′ Cy-5 modified 20 mers, 50 μM in deionized H_2O), spotted around transistors 30, 60, and 90). (Top) Microfluorescence image of the three DNA spots. Fluorescence intensity is given by the gray scale on the right.

initial charge of the SiO_2/poly(L-lysine)/electrolyte interface. Within the experimental peak-to-peak reproducibility, nonmodified (from four different commercial sources) and Cy-5 modified oligonucleotides give the same electronic signal.

After microspotting, we currently obtain reproducible detection of DNA for surface concentrations above 4 bases/nm^2. This estimation is based on the assumption that all molecules present in the 0.25-nl volume of a typical microspot (ϕ=100 μm, 10 μM, oligo 20mer) are immobilized on the poly(L-lysine) layer and contribute to the electronic signal. In weight units, this corresponds to 16.5 pg of DNA in the spot and 50 fg on the 24-μm^2 active surface of one FET.

To demonstrate electronic detection of double stranded (ds) DNA, we setup two polymerase chain reaction (PCR) tubes, A and B. Tube A is prepared for enzymatic amplification of a DNA fragment, 1009 base pairs in length. Initially, reference tube B has the same content as tube A, except that one of the four nucleotides is missing (dTTP replaced by dCTP to conserve the total dNTP concentration) to inhibit the synthesis of the ds-DNA product. Tubes A and B are thermocycled in parallel and are purified twice on spin columns (QIAGEN) to eliminate nucleotides, primers, proteins, and salt. After the purification, tube A is thus expected to contain, in addition to the content of tube B, PCR synthesized double-stranded DNA. By gel electrophoresis we estimate a DNA concentration of ~20 ng/μl in tube A (Fig. 11, inset).

With a micropipet we then deposit 0.15 μl of tube A and B on separate parts of a FET array. The array has previously been coated with poly(L-lysine) for DNA immobilization and measured for reference as described above. In the case of Fig. 11, the left part of the array has been covered with solution A, the right part with solution B, and the central part has been left untreated. We incubate 15 min without drying, rinse with water, and subsequently measure the current-voltage characteristics of the FET array. As expected, we observe that the FET's exposed to the DNA containing solution A exhibit sizeable negative shifts ΔU_S, while the FET's exposed to the reference solution B show no significant shifts.

All the electronic measurements presented in this paper were performed with an electrolyte solution on the transistor arrays leading to a detection of the surface attached biomol-

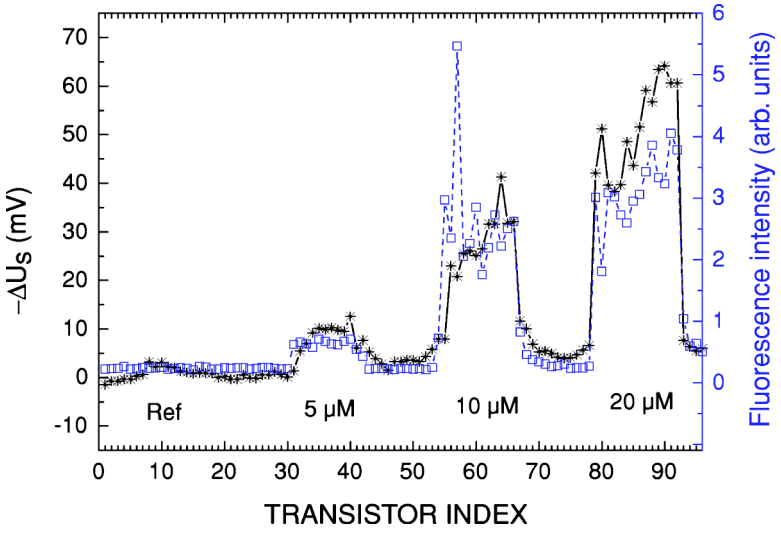

FIG. 10. Electronic and fluorescence detection of Cy5-modified oligonucleotides. Stars are derived from two electronic measurements performed before and after the four local deposits. They show the negative shift $-\Delta U_S$ of the transistor characteristics, induced by the DNA deposition. Open squares give the fluorescence intensity measured in air on the dry FET's after the electronic measurement.

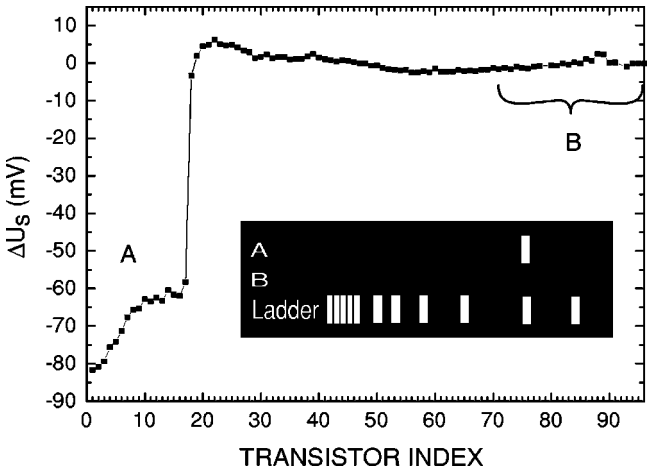

FIG. 11. Detection of nonfluorescent double stranded DNA after macroscopic deposition. The macrospots are incubated 15 min without drying, rapidly rinsed with water, and then covered with a common electrolyte ([KCl]=0.01 mM) for the electronic measurements. FET's 1–20 incubated with solution A containing PCR products are shifted downward compared to the central part of the array that has not been incubated. Reference solution B incubated on the right induces no significant shift. Inset: Agarose gel electrophoresis of the purified PCR products. From top to bottom: tube A, tube B, DNA weight marker (1-kB ladder, Promega).

ecules in an aqueous environment. Nevertheless, between local deposition and electronic measurements the adsorbed layers often go through drying, which might appear as an invasive change in the local molecular environment that could induce damage. However, local spotting of DNA on dried poly(L-lysine) layers with subsequent DNA drying is a common strategy for the preparation of DNA chips on glass and SiO_2 substrates [22,23]. After rehumidification specific hybridization is systematically achieved on such samples, showing that damage to the attached molecules is weak. We verified by fluorescence measurements that the DNA oligonucleotides immobilized on the transistor surfaces allow for subsequent specific hybridization. Furthermore, measurements performed without DNA drying (see, for instance, Fig. 11) show electronic signals that are comparable to the ones observed on dried samples.

VI. CONCLUDING REMARKS

In this work, silicon semiconductor devices with multiple transistor structures have been used for biomolecule detection. An active structure with dc readout potentially allows for a high level of miniaturisation, because its signal does not decrease with sensor surface and the simple dc measurement requires minimum space if on-chip readout electronics is envisaged. High-density, bidimensional FET arrays with on-chip readout electronics for sensor applications have recently been fabricated by silicon complementary metal-oxide semiconductor technology [24]. Cui *et al.* [5] reported the detection of biological and chemical species (but not DNA) by measuring conductance changes of individually connected, boron doped, silicon nanowires (~2 nm in diameter). These very small sensors underline the potential for miniaturization of the FET approach.

Passive field-effect devices, like Si/SiO_2 capacitors require larger sensor surfaces than FET's, because below a limit of about $50\times50\ \mu m^2$, the capacitive signal is dominated by the amplifier input capacitance and other stray capacitances that typically amount to a few pF [9]. Souteyrand *et al.* presented field effect detection of the hybridization of homo-oligomer DNA sequences on Si/SiO_2 capacitors and also some results obtained with an individual large area field-effect transistor [4]. More recently, Fritz *et al.*, demonstrated specific detection of hybridization between DNA oligonucleotides [6], using two microfabricated silicon cantilevers (500 μm long, 75 μm wide), each carrying a capacitive Si/SiO_2 sensor at the terminus.

In our measurements, the noise of the FET's presently does not represent a limiting factor (effective noise in U_S is below 100 μV for an acquisition time of 3 ms per data point). A more important difficulty is the sensitivity to gradual changes at the interface (biomolecule desorption, variations in *p*H and salt). For instance, the limit of detection in spotting experiments is often given by parasite signals induced by buffer drying, as examplified in Figs. 8 and 10. The differential measurement helps, since it allows us to be insensitive to rigid drift, as for example temporal drifts in U_S caused by a gradual change in the interface state of the whole array (between ±0.02 mV/min and ±2 mV/min depending on manipulations). Two measurements, separated by a 15 min interval and intermediate H_2O rinsing often appear shifted by up to 15 mV (measurements on 99 poly-lysine coated arrays statistically give a shift by -0.2 ± 22 mV), the FET-to-FET variation is, however, typically an order of magnitude smaller.

The planar surface of the array is an attractive feature, since microfluidics devices fabricated from polymers [25], plastics or glass [26] are usually flat and could be attached by adhesion or thermal bonding to the silicon chip. In fact, one of us has already shown that polymer structures of up to 50 μm in height can be processed on the devices without perturbing the function of the FET arrays [11]. Future work could thus be oriented towards integration with microfluidics based "lab on a chip" techniques and analysis of complex DNA in microarray format. In addition, our approach may become a useful tool for studying enzyme activities, as the latter are often associated with charge variation.

ACKNOWLEDGMENTS

We would like to thank P. Fromherz for continuous support. L.P.A. is associated with the CNRS and the universities Paris VI and VII.

APPENDIX: MICROFLUORESCENCE

Our setup for spatially resolved fluorescence measurements is based on an upright optical microscope (Olympus BX50 WI). A HeNe laser beam is expanded by a telescope, is introduced in the microscope illumination path and is focused with a microscope objective (Olympus, UPlanFL

10×, N.A. 0.3) to a spot of adjustable diameter (0.5–10 μm). Local fluorescence is collected by the same objective and passes through two piezoadjustable slits (Piezosystem Jena, PZS1) positioned in two separate image planes in crossed orientation. The two-slit arrangement defines the detection region on the sample (like the pinhole in more standard confocal arrangements) and allows us to optimize this region with respect to the size of the excitation spot. Excitation light is blocked by appropriate dichroic beamsplitter and emission filter and light detection is performed with a peltier-cooled photomultiplier tube in photon counting mode (Hamamatsu H7421-40). A motorized *xy* translation stage (Newport VP-25XA) with integrated position sensors and operating in a computer-adjustable feedback loop allows us to scan the sample over 25×25 mm with 0.2-μm repeatability.

[1] P. Bergveld, IEEE Trans. Biomed. Eng. **19**, 342 (1972).
[2] P. Bergveld, Sens. Actuators, A **56**, 65 (1996).
[3] A. B. Kharitonov, J. Wassermann, E. Katz, and I. Willner, J. Phys. Chem. B **105**, 4205 (2001).
[4] E. Souteyrand, J. P. Cloarec, J. R. Martin, C. Wilson, I. Lawrence, S. Mikkelsen, and M. F. Lawrence, J. Phys. Chem. B **101**, 2980 (1997).
[5] Y. Cui, Q. Wei, H. Park, and C. M. Lieber, Science **293**, 1289 (2001).
[6] J. Fritz, E. B. Cooper, S. Gaudet, P. K. Sorger, and S. R. Manalis, Proc. Natl. Acad. Sci. U.S.A. **99**, 14142 (2002).
[7] F. Pouthas, C. Gentil, D. Côte, and U. Bockelmann, Appl. Phys. Lett. **84**, 1594 (2004).
[8] J. R. MacDonald, *Impedance Spectroscopy* (Wiley, New York, 1987).
[9] R. Wiegand, K. R. Neumaier, and E. Sackmann, Rev. Sci. Instrum. **71**, 2309 (2000).
[10] V. Kiessling, B. Müller, and P. Fromherz, Langmuir **16**, 3517 (2000).
[11] G. Zeck and P. Fromherz, Proc. Natl. Acad. Sci. U.S.A. **98**, 10457 (2001).
[12] J. Persello, in *Adsorption on Silica Surfaces*, edited by E. Papirer, Surfactant Science Series No. 90 (Marcel Dekker, New York, 2000), p. 297, Table 8.
[13] A. J. Bard and L. R. Faulkner, *Electrochemical Methods, Fundamentals and Applications* (Wiley, New York, 1980).
[14] I. Larson and P. Attard, J. Colloid Interface Sci. **227**, 152 (2000).
[15] *CRC Handbook of Chemistry and Physics*, 75th ed., edited by D. R. Lide (CRC Press, Boca Raton, FL, 1994).
[16] Although at large U_{SD} the electric field E_{SiO_2} changes from source to drain, the potential at the oxyde/electrolyte interface remains approximately constant because of lateral screening by mobile ions. See, for example, Ref. [17]. Therefore the model remains one dimensional in the electrolyte, where all variations of potential drops occur at fixed working point $\{I_D, U_{SD}\}$.
[17] C. D. Fung, P. W. Cheung, and W. H. Ko, IEEE Trans. Electron Devices **33**, 8 (1986).
[18] R. A. Latour, S. D. Trembley, Y. Tian, G. C. Lickfield, and A. P. Wheeler, J. Biomed. Mater. Res. **49**, 58 (2000).
[19] J. K. West, R. Latour and L. L. Hench, J. Biomed. Mater. Res. **37**, 585 (1997).
[20] P. Sens and J. Joanny, Phys. Rev. Lett. **84**, 4862 (2000).
[21] G. Decher, Science **277**, 1232 (1997).
[22] M. B. Eisen and P. O. Brown, Methods Enzymol. **303**, 179 (1999).
[23] R. Sinibaldi, C. O'Connell, C. Seidel, and H. Rodriguez, Methods Mol. Biol. **170**, 211 (2001).
[24] B. Eversmann, M. Jenkner, F. Hofmann, C. Paulus, R. Brederlow, B. Holzapfl, P. Fromherz, M. Merz, M. Brenner, M. Schreiter, R. Gabl, K. Plehnert, M. Steinhauser, G. Eckstein, D. Schmitt-Landsiedel, and R. Thewes, IEEE J. Solid-State Circuits **38**, 2306 (2003).
[25] Y. Xia and G. M. Whitesides, Angew. Chem., Int. Ed. **37**, 550 (1998).
[26] E. T. Lagally, P. C. Simpson, and R. A. Mathies, Sens. Actuators B **63**, 138 (2000).